ORIENTAL JOURNAL OF CHEMISTRY
An International Open Access, Peer Reviewed Research Journal
www.orientjchem.org
ISSN: 0970-020 X
CODEN: OJCHEG
2024, Vol. 40, No.(6):
Pg. 1723-1735

Eco-friendly and Sustainable Biosynthesis of ZnO Nanomaterials for Photocatalytic Degradation of Industrial Effluent Under Natural Sunlight

SANA MOHD SALIM SHAIKH[1]*, MANISH SHAMRAO HATE[2] and RAMESH CHAUGHULE[3]

[1,2,3]Ramnarain Ruia Autonomous College, Department of Chemistry, Matunga, Mumbai, Maharashtra, India.
*Corresponding author E-mail: sanashaikh@ruiacollege.edu

http://dx.doi.org/10.13005/ojc/400625

(Received: August 12, 2024; Accepted: November 04, 2024)

ABSTRACT

This study investigates the synthesis, characterization, and use of zinc oxide nanoparticles (ZnONPs) for degrading water sample from a common effluent treatment plant (WSCETP) and a specific industrial source (Water Sample from Padmaja Laboratories, abbreviated as WSPL). zinc oxide nanoparticles were produced through a green microwave-assisted approach with *Moringa Oleifera* Lam and analysed using various spectroscopic and microscopic techniques. UV-Visible spectroscopy identified a peak at 308 nm and a band gap of 3.06 eV. Fourier Transform Infrared Spectroscopy confirmed Zn-O stretching and various organic groups. X-ray diffraction analysis indicated a hexagonal wurtzite structure with a crystal size of 21 nm, while Field Emission Scanning Electron Microscopy and Energy Dispersive X-ray Spectroscopy revealed a uniform, spherical morphology, and high purity. Photocatalytic tests showed optimal Chemical Oxygen Demand reductions at 7.5 g/L for Water Sample from Common Effluent Treatment Plant and 10 g/L for Water Sample from Padmaja Laboratories, with pH values of 8.2 and 8.0, respectively. Recyclability tests demonstrated significant activity retention, with Chemical Oxygen Demand reductions of 18% and 62% after four cycles for Water Sample from Common Effluent Treatment Plant and Water Sample from Padmaja Laboratories, respectively. Zinc oxide nanoparticles are effective, recyclable, providing a cost-efficient method for industrial effluent treatment.

Keywords: Green synthesis of Zinc oxide nanoparticles, Photocatalytic effluent degradation, Industrial wastewater treatment, Chemical Oxygen Demand reduction, Catalyst recyclability.

INTRODUCTION

Effluent, the wastewater released from industrial, agricultural, or domestic activities, often contains a complex mix of contaminants, including heavy metals, organic pollutants, and pathogens. The effective treatment of effluents is crucial to mitigate their adverse impact on ecosystems and human health. Traditional treatment methods encompassing physical, chemical, and biological approaches are widely used for contaminant removal and regulatory compliance, but each method faces limitations in either efficiency or sustainability when scaled up[1-3].

Nanotechnology, particularly the use of zinc oxide (ZnO) nanoparticles, has recently gained

attention as a promising solution for enhancing wastewater treatment. ZnO nanoparticles are valued for their high photocatalytic activity, chemical stability, and broad-spectrum antibacterial properties, making them effective in degrading organic pollutants and disinfecting wastewater[4]. Due to their direct and wide bandgap and high exciton binding energy, ZnO nanoparticles efficiently absorb UV-light, generating reactive oxygen species that break down pollutants[5]. However, conventional ZnO nanoparticle synthesis methods often involve hazardous chemicals and energy-intensive processes, which can pose environmental and health risks. To address these concerns, green synthesis techniques have emerged, utilizing plant extracts and other biological agents as reducing agents to create ZnO nanoparticles in a more sustainable manner.

Moringa oleifera Lam, commonly known as the drumstick tree, is a compelling green synthesis agent for ZnO nanoparticles. Compared to other sources like Aloe vera or *Azadirachta indica* (neem), *Moringa* leaves contain a unique array of bioactive compounds, including polyphenols, flavonoids, and antioxidants, which facilitate the efficient reduction and stabilization of zinc ions. These compounds contribute to uniform nanoparticle size and improved stability, which are critical factors in enhancing catalytic performance. Additionally, *Moringa* is widely available, cost-effective, and easily cultivated, making it a practical choice for scalable and environmentally friendly nanoparticle production.

In this study, we used *Moringa oleifera* Lam leaves for the biosynthesis of ZnO nanoparticles and evaluated their structural and optical properties, focusing on their effectiveness in treating industrial effluents. Natural sunlight was selected as the energy source for photocatalytic degradation, providing a sustainable alternative to artificial UV sources. Sunlight contains a broad spectrum of light, including UV, Visible, and infrared components, enhancing the practical applicability of this method. Although ZnO nanoparticles exhibit optimal photocatalytic performance in the UV range, natural sunlight's inclusion of UV wavelengths makes it an efficient, eco-friendly option for large-scale applications without the need for additional energy input.

This approach aligns with real-world conditions, where natural sunlight can be harnessed to maximize photocatalytic degradation, offering a viable, sustainable solution for wastewater treatment. By leveraging *Moringa's* bioactive compounds and the energy from sunlight, this study aims to contribute to scalable, green methodologies that improve wastewater management while reducing the environmental footprint associated with conventional nanoparticle synthesis and effluent treatment processes.

Table 1: Comparative Analysis of Nanomaterials Used in Effluent Treatment

Nanomaterial	Synthesis method	Type of effluent	Light source used	%Degradation	Treatment Time (minutes)	References
ZnO-Ag	Green synthesis (bacteria)	Dairy wastewater	UV-light	98%	100 min	[9]
Graphene oxide	Chemical exfoliation	Heavy metal contaminated water	Sunlight	88%	140	[12]
Fe_3O_4	Co-precipitation	Pharmaceutical wastewater	UV-light	80%	150	[14]
ZnO	Sol-Gel	Industrial wastewater	UV-C light	95%	120	[17]
Au	Green synthesis	Municipal wastewater (algae)	Visible-light	87%	190	[19]
Ag	Green synthesis (plant extract)	Hospital wastewater	Visible-light	85%	180	[24]
TiO_2	Hydrothermal	Textile dye effluent	Sunlight	90%	240	[28]

EXPERIMENTAL

Materials

Moringa oleifera Lam. twigs having leaves were collected from Samudranand Siddhasthal, Manori Village, Malad (W.), [Latitude:19.1978°N Longitude: 72.7920°E, Temperature 29°C, Humidity 76%] Mumbai, Maharashtra, India, on 21st January 2023 at 4.00 pm in the evening. The leaves were separated from the twigs and then washed properly and kept for shed drying for almost 15 to 16 days. The plant material was initially ground into a powder using an electric mixer grinder, then sieved through a mesh with a number 75, and stored at RT. The plant was authenticated by the Agharkar Research Institute, Pune, Maharashtra, India.

All chemicals utilized for synthesis of ZnONPs were of A.R. grade and were employed without additional purification. Zinc nitrate hexahydrate and ethanol were obtained from Merck Chemicals Pvt. Ltd., India, while acetic acid and ammonia were supplied by S.D. Fine Chemicals Limited, India, for adjusting pH. Additional reagents included $K_2Cr_2O_7$, KI, mercuric sulphate, manganese sulphate, sodium azide, sodium thiosulfate, silver sulphate, starch, ferrous ammonium sulphate, ferroin indicator, and A.R. H_2SO_4 were all purchased from S.D. Fine Chemicals Limited, India. Double distilled water was utilized in all experiments.

Effluent samples were collected from Padmaja Aerobiologicals Pvt. Ltd., Turbhe, Navi Mumbai, and from the equalization tank of CETP (Thane-Belapur) association, Navi Mumbai. The samples, collected without preservatives, were analysed within 24 h of collection and stored at room temperature within two to three hours. Any suspended matter was removed by filtration using Whatman filter paper No. 41.

Synthesis of ZnONPs

The leaf extract of *Moringa oleifera* Lam. was prepared using Soxhlet extraction. Five grams of dried leaf powder were placed in the Soxhlet apparatus, and 250 mL of anhydrous ethanol was added as the solvent. The extraction was conducted at a temperature of 80°C, which is slightly above the boiling point of ethanol (78.5°C), allowing for efficient extraction of the desired compounds from the leaf material. The Soxhlet apparatus facilitated continuous reflux, ensuring that the ethanol vaporized, condensed, and re-extracted the compounds from the leaf powder repeatedly over a duration of 18 hours. After the extraction process was complete, the mixture was filtered through Whatman filter paper No. 42 to separate the leaf residue from the ethanol extract. In the synthesis procedure, 1.487 g of $Zn(NO_3)_26H_2O$ was mixed with 10 mL of the extract with continuous stirring. The solution was subjected to microwave irradiation (Microwave Oven, Samsung 20L Solo, MW73AD-B/XTL) for 1 min at 1150 W. This resulted in a yellow precipitate, indicating the development of $Zn(OH)_2$. Distilled water was used to rinse the precipitate twice subsequently followed by ethanol, then dried at 100°C for 1 hour. It was finally calcined in a muffle furnace at 600°C for 2 h to yield ZnONPs.

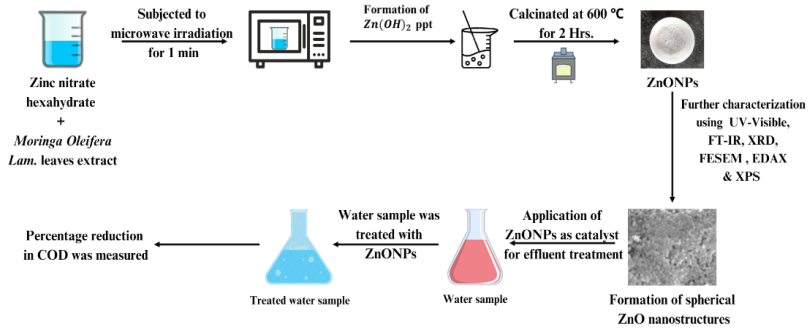

Fig. 1. Work flow representing synthesis of ZnONPs used for effluent treatment. (Original work by the author)

Characterization

The ZnONPs were characterized using several methods. UV-Vis spectrophotometer (Shimadzu UV-Visible Spectrophotometer 1800) was used to assess the optical properties over a range of 200-800 nm in aqueous dispersion, and the band gap was calculated. Perkin Elmer FT-IR was employed to identify functional groups within the 4000-500 cm^{-1} range. The atomic arrangement was analysed using an Japan Rigaku Smart Lab, X-ray diffractometer with monochromatic CuKα radiation ($\lambda = 0.15406$ nm) over a 2θ range of 30 to 75 degrees. Surface morphology was identified with Carl Zeiss Model Supra 55, Germany, FESEM equipped with EDAX at a 20 kV accelerating voltage.

Sample preparation

The collected wastewater samples were very concentrated. To adjust the values to a manageable range, the WSCETP sample was diluted in a 1:1 ratio, while the WSPL sample was diluted at a 1:10 ratio using double distilled water. The initial pH of each sample was then measured.

Photocatalytic degradation of effluents

In a typical process for both effluents

(WSCETP & WSPL), a fixed amount of photocatalyst was suspended in 1L of effluent and left in a dark environment for several hours to achieve absorption-desorption equilibrium. Subsequently, the solution was then magnetically stirred to keep the catalyst uniformly suspended and exposed to sunlight. Samples were withdrawn at regular intervals to monitor degradation, which was assessed by measuring the absorbance spectrum using a Shimadzu UV-Visible (1800) Spectrophotometer, and by evaluating the percentage reduction in COD.

Analysis of raw and treated effluents

The WSCETP sample was deep blue, while the WSPL sample was orange. Both effluent samples, before and after treatment with ZnONPs, were analysed for key quality parameters, including BOD, COD, TDS, TS and TSS as per the methods specified under the standard guidelines for water and wastewater examination.

RESULTS

Characterization of ZnONPs

UV-Visible Spectroscopy

The UV-Visible absorption spectrum, shown in Fig. 2(a), exhibits a distinct peak around 308 nm, indicative of the intrinsic band-gap absorption of ZnONPs. This peak represents electron transitions from the valence band to the conduction band, indicating strong optical absorption in the UV region, which is characteristic of the wide band gap of ZnO. The Tauc plot in Fig. 2(b) was employed to determine the optical band gap of the ZnONPs, with the extrapolated band gap energy determined to be approximately 3.06 eV. This value is near to the typical band gap of bulk ZnO (around 3.2 eV), with the minor difference potentially due to quantum confinement effects from the nanoparticle size. A band gap of 3.06 eV enables ZnONPs to effectively absorb UV light and generate electron-hole pairs. These pairs can migrate to the surface and engage in redox reactions, resulting in the formation of reactive oxygen species (ROS).

In effluent treatment, the generation of ROS on the nanoparticle surface is essential for degrading organic pollutants and inactivating microbial contaminants. ROS-induced oxidative stress can damage microbial cell membranes and disrupt metabolic processes, aiding in the disinfection of wastewater. Additionally, ZnONPs photocatalytic activity can degrade complex organic molecules into simpler, less harmful substances, enhancing the overall effectiveness of effluent treatment.

Fourier Transform Infrared spectroscopy

The FTIR spectrum, illustrated in Fig. 2(c), reveals several distinct peaks. The peaks at 891 cm^{-1} and 662 cm^{-1} correspond to Zn-O stretching vibrations, which confirm the presence of ZnONPs, recognized for their photocatalytic properties. Peaks at 3465 cm^{-1} and 3007 cm^{-1} are linked to O-H stretching vibrations, indicating the presence of hydroxyl groups, possibly from absorbed water or surface hydroxylation, which enhance the nanoparticles capability to generate reactive oxygen species for pollutant degradation. A peak at 2325 cm^{-1} suggests the presence of CO_2, likely adsorbed from the atmosphere. The peak at 1734 cm^{-1} corresponds to C=O stretching vibrations, potentially indicating the existence of organic residues or carbonate species on the nanoparticle surface. Peaks at 1361 cm^{-1} and 1147 cm^{-1} are associated with C-H bending and C-O stretching vibrations, suggesting the presence of organic compounds. These observations imply that the Moringa oleifera leaf extract used during synthesis contributes organic functional groups that can stabilize the nanoparticles. While the treatment at 600°C may degrade some organic compounds, it is plausible that certain organic groups, especially those strongly bonded to the ZnO surface, can persist due to their interaction with the metal oxide. This stability of functional groups enhances the efficiency of the synthesized ZnONPs in effluent treatment by facilitating the breakdown of organic contaminants and improving water quality[6-7].

X-ray diffraction analysis

Figure 2(d) presents the XRD pattern obtained for ZnONPs. The diffraction peaks identified at 2θ angles of 31.58°, 34.25°, 36.07°, 47.37°, 56.44°, 62.72°, 66.24°, 67.82°, and 69.02° correspond to the following (100), (002), (101), (102), (110), (103), (200), (112), and (201) crystallographic planes of the hexagonal wurtzite structure of ZnONPs with space group P63mc, as indexed in the Crystallography Open Database (COD) entry 9011662. The sharp and distinct peaks indicate good crystallinity of the ZnONPs. The absence of any additional peaks indicates the phase purity of ZnO, with no secondary phases detected. The mean crystal size of the nanoparticles, calculated by applying the Debye-Scherrer equation and was determined to be 21 nm.

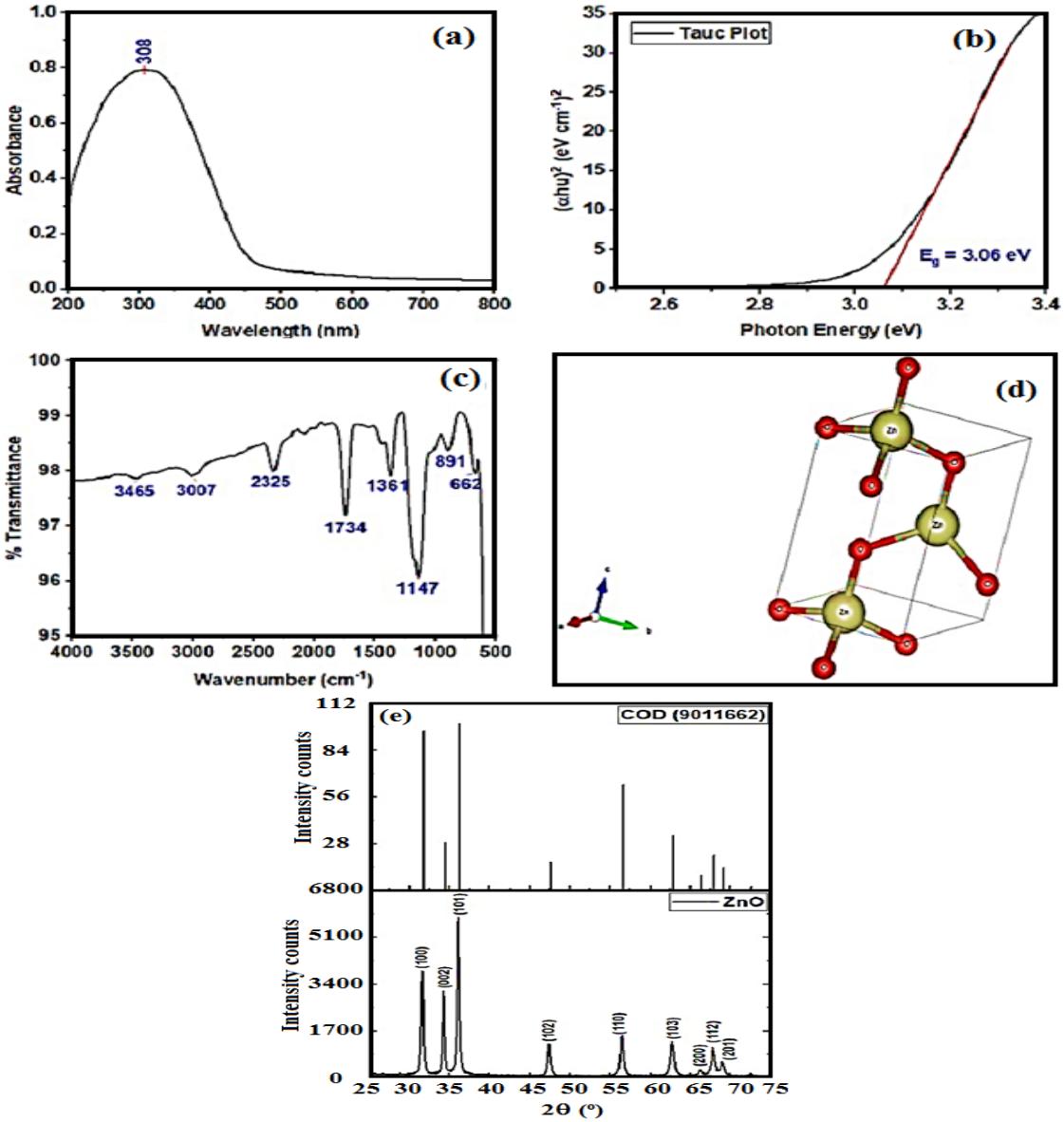

Fig. 2(a). UV Visible spectrum, (b) Tauc plot result, (c) FTIR spectrum, (d) Unit cell structure (e) XRD pattern of ZnONPs. (Original work by the author)

Field Emission Scanning Electron Microscopic Studies with Energy Dispersive Analysis of X-rays

The morphology of the synthesized ZnONPs was examined using FESEM. As depicted in Fig. 3 (a-d), the FESEM images reveal that the ZnONPs have a porous and rough surface texture with a generally homogeneous structure. Some agglomeration was observed, which is common in nanoparticle systems, but no other predominant phases were detected. The nanoparticles predominantly exhibit a spherical-like shape, indicating uniform synthesis.

To confirm the formation of ZnONPs and assess their elemental composition, EDAX analysis was performed. The EDAX spectra, displayed in Fig. 4(a), confirmed the presence of Oxygen (O) and Zinc (Zn) atoms, matching the expected composition. The elemental composition by weight percentage was 81.62% Zinc and 18.38% Oxygen, reflecting a slight deviation from the stoichiometric ratio but still within an acceptable range for ZnO nanoparticles. The particle size distribution curve as depicted in Fig. 4(b) displays a mean particle size of 25 nm.

The FESEM-EDAX analysis indicates that the synthesized ZnONPs are of high purity, as no other elements were detected. The EDS mappings of the ZnONPs, shown in Fig. 4(c-d), further verify that Zinc and Oxygen are the main elements in the nanoparticles. The spatial distribution of these elements aligns well with the SEM images, confirming the uniformity and homogeneity of the ZnONPs. These characteristics make the ZnONPs well-suited for applications in effluent treatment, especially in photocatalytic degradation processes, where particle size, purity, and surface properties are critical.

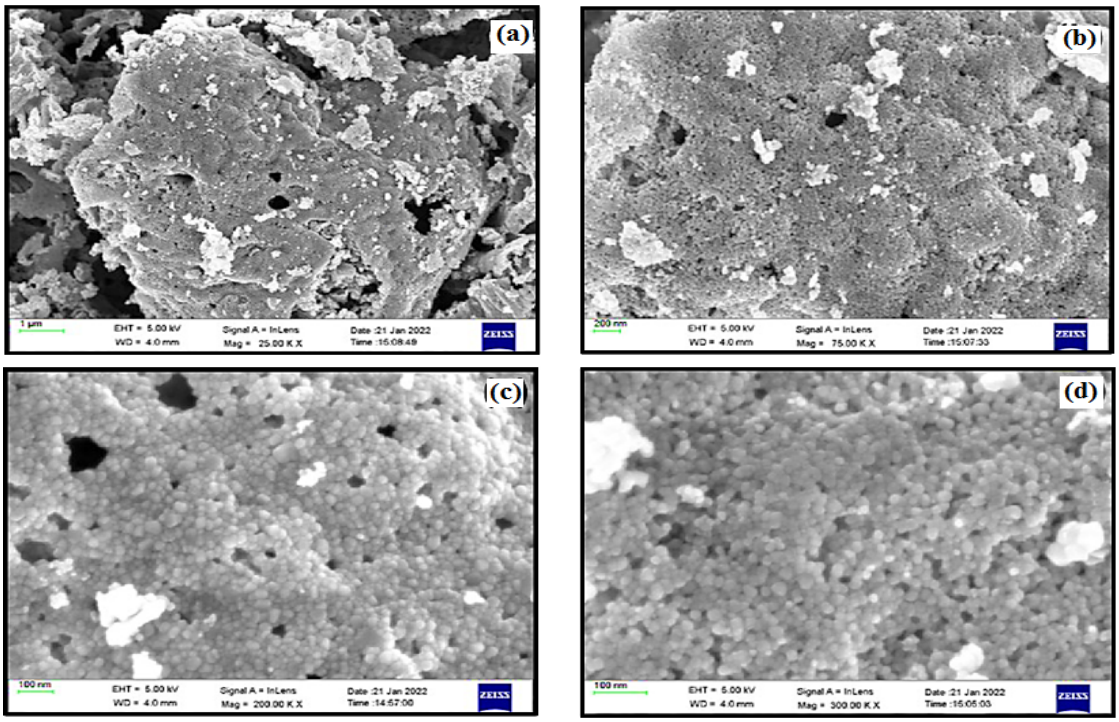

Fig. 3(a-d). FESEM image (different magnifications) of ZnONPs. (Original work by the author)

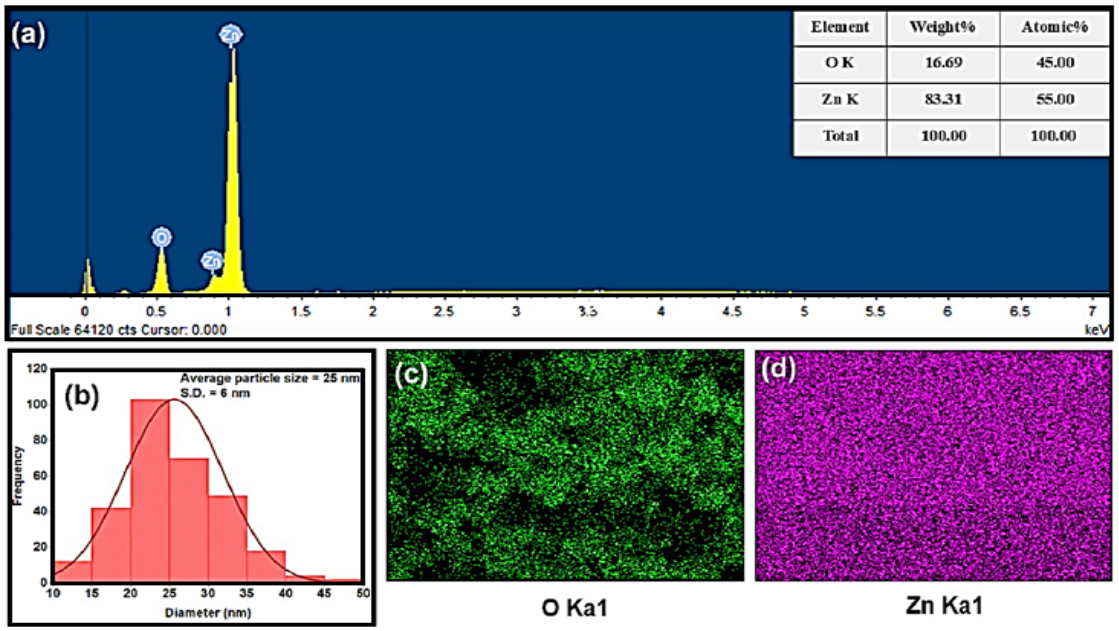

Fig. 4(a). EDAX spectrum, (b) Particle size distribution, (c-d) EDS mapping of composition of ZnONPs. (Original work by the author)

Analysis of raw effluent samples

The raw effluent samples were assessed for key quality parameters, with the results indicated in Table 3. The findings indicate that the effluents were highly polluted, had low biodegradability, and required pre-treatment before discharge to avoid significant environmental harm.

UV-Vis spectrum of the raw effluent samples

The UV-Vis spectra of the raw effluents from WSCETP and WSPL, shown in Fig. 5(a) and 5(b), reveal numerous peaks in both the UV and visible regions. The raw WSCETP sample displays high absorbance in the 200-350 nm range, with notable peaks around 250 nm, indicating a significant presence of organic compounds. The raw WSPL sample shows even higher absorbance, especially between 200-400 nm with peaks around 230-240 nm, suggesting a higher concentration of organic compounds, likely due to industrial processes. This suggest that the effluent sample contains diverse organic chromophoric compounds. The reduced biodegradability values for these effluents (WSCETP: BOD_5/COD = 0.26-0.30; WSPL: BOD_5/COD = 0.24-0.26) support this observation, emphasizing the need for effective treatment to achieve complete mineralization.

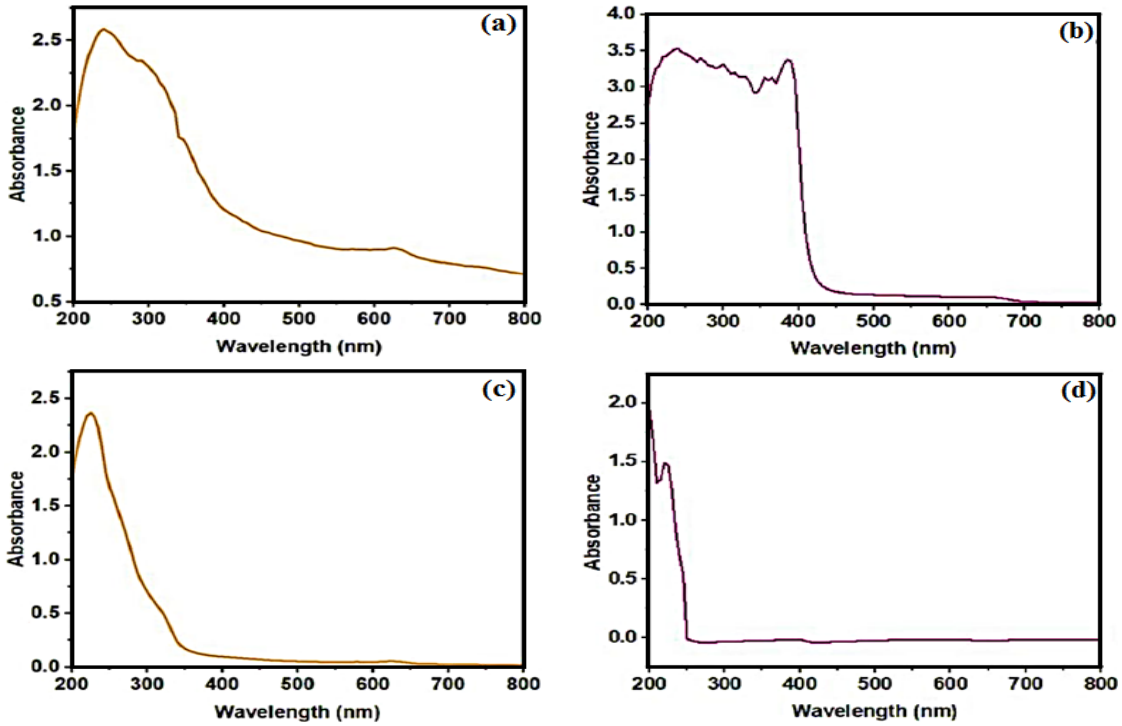

Fig. 5. Absorption Spectrum of the Raw Effluents (a) WSCETP and (b) WSPL and treated effluents (c) WSCETP and (d) WSPL. (Original work by the author)

Photocatalytic treatment of the effluents under Sunlight

The effluents were exposed to sunlight with ZnONPs acting as the photocatalyst. The process variables like catalyst concentration and starting pH were fine-tuned to assess the impact of ZnONPs addition.

Effect of catalyst dose

Figure 6 depicts the COD reduction of effluents over time when exposed with ZnONPs at different catalyst loadings. The study involved varying the catalyst loading up to 12.5 g/L for WSCETP and 20 g/L for WSPL under sunlight irradiation. COD reduction was monitored every 30 min for 3 h for WSCETP and every hour for 4 h for WSPL. COD, a key water quality indicator, measures organic pollutants; lower COD values indicate better pollutant degradation.

For WSCETP, the highest COD reduction of 32% was achieved with a catalyst concentration of 7.5 g/L, reducing COD from 600 mg/L to 404 mg/L over 3 hours. Increasing the catalyst loading beyond 7.5 g/L did not significantly reduce the COD, suggesting that 7.5 g/L is the optimal

amount. The modest COD reduction is attributed to the prior treatment of WSCETP, which left fewer organic pollutants for further degradation.

In comparison, WSPL showed a more significant COD reduction of 78% with a catalyst concentration of 10 g/L, decreasing COD from 1250 mg/L to 269 mg/L within 4 hours. This higher reduction is due to the greater initial COD in WSPL, indicating more organic pollutants available for degradation. Similar to WSCETP, increasing the catalyst loading beyond 10 g/L did not notably enhance COD reduction, making 10 g/L the optimal loading for WSPL.

For both effluents, majority of the COD reduction occurred inside the initial hours of treatment, highlighting the rapid catalytic activity of ZnONPs. The study concludes that ZnONPs are highly effective in reducing COD, especially in effluents with elevated organic content, and emphasizes the significance of optimizing catalyst loading to achieve maximum degradation efficiency while minimizing material use. The optimal catalyst loadings of 7.5 g/L for WSCETP and 10 g/L for WSPL were used in subsequent experiments to investigate the impact of pH on effluent degradation.

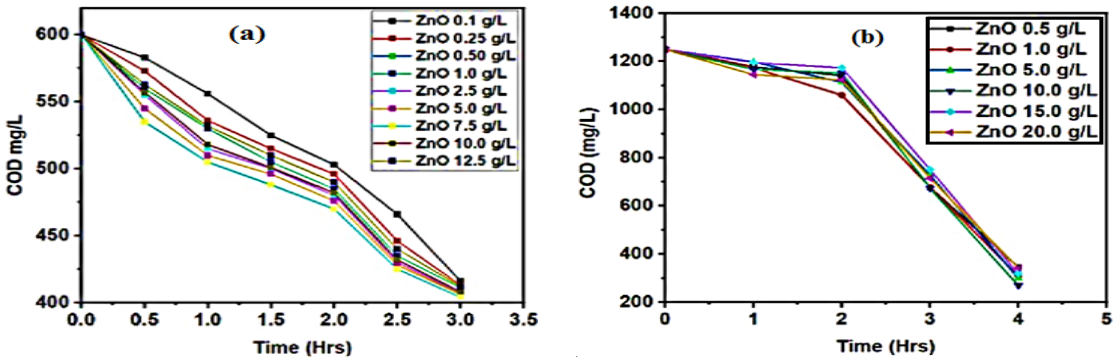

Fig. 6. Reduction in COD for the effluents: (a) WSCETP and (b) WSPL, at various catalyst loadings

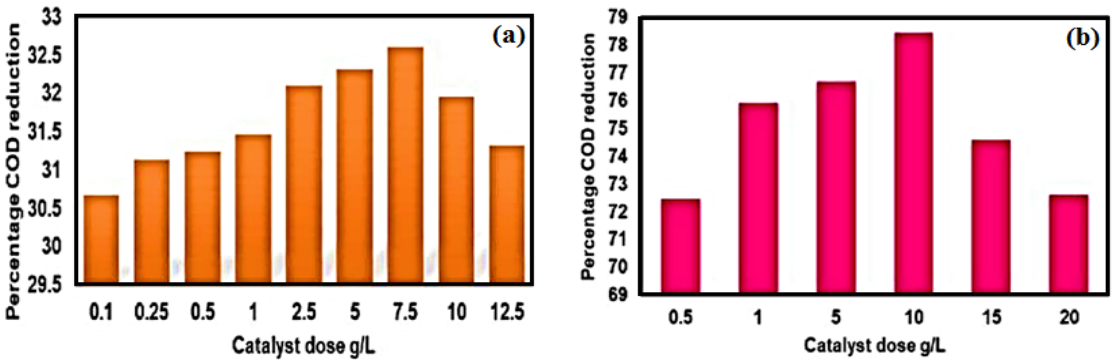

Fig. 7. Percentage reduction in COD for the effluents: (a) WSCETP and (b) WSPL, at various catalyst loadings over a 3-h period. (Original work by the author)

Effect of pH

The investigation focused on the role of pH in the photocatalytic breakdown of industrial effluents (WSCETP and WSPL) using ZnONPs. pH is crucial as it affects the effluent characteristics and hydroxyl radical production during photocatalysis. It influences ZnO activity by modifying particle charge, aggregate size, and the positioning of conduction and valence bands, thereby impacting photocatalytic efficiency, especially for charged substrates.

Photocatalytic degradation tests were performed across a range of initial pH values from 4 to 10.4 to determine the final pH and COD reduction percentage after treatment. pH adjustments were made using 0.02N H_2SO_4 or 0.02N NH_3 solutions.

The results indicated that for WSCETP, the optimal COD reduction occurred at a start pH of 8.2, yielding an end pH of 7.2 and a 30% COD reduction. This final pH is suitable for subsequent biological treatment, which requires a neutral pH for effective biodegradation. For WSPL, the best results were achieved at an initial pH of 8.0, resulting in an

end pH of 7.4 and a 76% COD reduction. This pH is also favourable for biological treatment, allowing for further mineralization.

Other pH levels, particularly those within the alkaline range, also showed favourable degradation rates, but achieving a final pH conducive to biological treatment was critical. The study concluded that initial pH values of 8.2 for WSCETP and 8.0 for WSPL are optimal for maximum COD reduction and preparation for subsequent biodegradation.

Table 2: Variations in pH and percentage COD Reduction values of effluents post-photocatalytic breakdown at various starting pH Levels

WSCETP			WSPL		
pH (BT)	pH (AT)	% COD reduction	pH (BT)	pH (AT)	% COD reduction
4.2	6.1	10	4.4	5.2	20
6.2	6.8	20	6.5	6.6	45
7.4	8.9	24	7.0	8.5	65
8.2	7.2	30	8.0	7.4	76
10.4	8.2	32	10.2	8.0	78

[Note: BT refers to before photocatalytic treatment and AT refers to after photocatalytic treatment.]

Properties of the effluent and absorption spectrum following photodegradation

The reaction parameters were fine-tuned to improve the economic efficiency of the degradation process. The properties of the effluents after photocatalytic breakdown using ZnONPs under sunlight were analysed, and the findings are summarized in Table 3. The BOD_5/COD ratio is commonly used to assess wastewater biodegradability. A ratio above 0.3 indicates better biodegradability, while a ratio below 0.3 suggests the wastewater is less biodegradable. The data in Table 3 show a substantial decrease in COD values after treatment, leading to a rise in the BOD_5/COD ratio from 0.26-0.30 to 0.64-0.67 for WSCETP and from 0.24-0.26 to 1.06-1.36 for WSPL. This suggests that effluents that were originally non-biodegradable turned biodegradable after undergoing photocatalytic process.

Table 3: Characteristics of effluent samples

Characteristics	WSCETP		WSPL	
	Value before treatment (mg/L)	Value after treatment (mg/L)	Value before treatment (mg/L)	Value after treatment (mg/L)
pH	10.8	7.2	3.5	7.4
COD	520-600	400 – 415	1150 – 1250	269 – 345
Total dissolved solids	3334	2976	270	128
Total suspended solids	386	0	50	0
Total solids	3720	2976	320	128
BOD_5/COD	0.26 - 0.30	0.64 – 0.67	0.24 – 0.26	1.06 – 1.36

Figures 5(c) and 5(d) display the UV-Vis spectra of the treated effluents over time following photocatalytic degradation under sunlight. After treatment with ZnO nanoparticles, both WSCETP and WSPL effluents exhibit a notable reduction in absorbance, particularly in the previously high-absorbance UV range. This reduction indicates that the ZnO nanoparticles have effectively degraded or removed a significant portion of the organic pollutants in the raw effluents. The substantial decrease in UV absorbance in both treated effluents confirms the efficacy of ZnO nanoparticles in improving the effluent quality, making it cleaner and less harmful.

Effect of recycling ZnO

Figure 8 highlights the recyclability and efficiency of ZnO nanoparticles (ZnONPs) as a catalyst for the degradation of WSCETP and WSPL effluents. Under experimental conditions of pH 8.2 with 7.5 g/L of ZnONPs for WSCETP and pH 8.0 with 10 g/L for WSPL, initial chemical oxygen demand (COD) reductions were approximately 32% and 78%, respectively. Recyclability tests indicated a gradual decline in efficiency over four cycles: for WSCETP, COD reduction dropped to around 30% after the first cycle and further to 18% by the fourth; for WSPL, it declined from 78% in the first cycle to approximately 62% by the fourth. This reflects a

decrease in efficiency of about 14% for WSCETP and 16% for WSPL over four cycles.

The observed reduction in catalytic activity across cycles may be attributed to several factors. Surface fouling or partial deactivation of ZnONPs can occur as organic residues and by-products accumulate on the catalyst surface, which may obstruct active sites and hinder photocatalytic performance. Additionally, some degree of nanoparticle aggregation during repeated use could lead to a decrease in effective surface area, thereby reducing overall efficiency. Minor changes in ZnONPs structural properties, such as alterations in crystallinity or oxidation states, may also contribute to the decline in activity. Despite this, ZnONPs still demonstrated significant COD reductions across multiple cycles, maintaining substantial photocatalytic performance, particularly in WSPL effluents. This ability to be reused for several cycles without drastic efficiency loss highlights ZnONPs as cost-effective and practical catalysts for wastewater treatment applications.

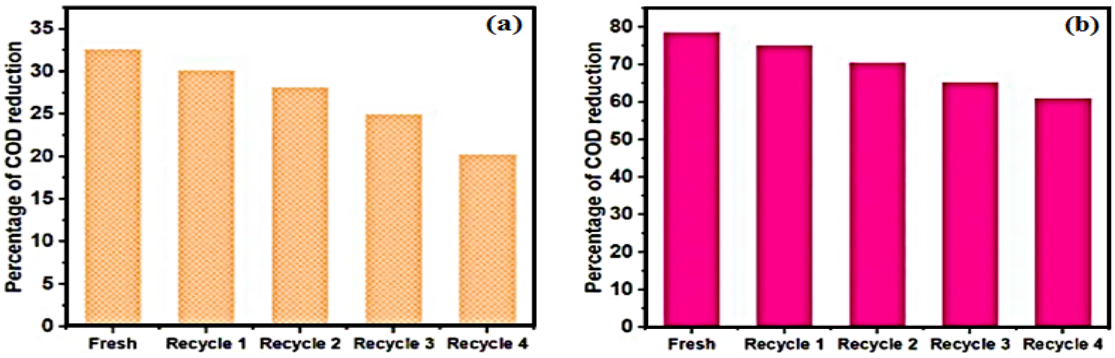

Fig. 8. Recyclability of ZnONPs for the degradation of (a) WSCETP and (b) WSPL effluents. (Original work by the author)

DISCUSSION

The synthesis of Zinc oxide nanoparticles (ZnONPs) from *Moringa oleifera* Lam and their subsequent application in photocatalytic degradation of industrial effluents present significant implications for environmental remediation. The utilization of *Moringa oleifera* as a green reducing agent is particularly noteworthy due to its abundant bioactive compounds, including phenolics and flavonoids, which not only facilitate the reduction of zinc ions but also enhance the photocatalytic properties of the synthesized nanoparticles. Moreover, *Moringa oleifera* is widely available, cost-effective, and eco-fri endly, making it an excellent candidate for the sustainable synthesis of nanoparticles[3,14].

The optimization of ZnO NPs loading in treating wastewater effluents, with an optimal catalyst loading of 14 mg/L for WSCETP effluent and 15 mg/L for WSPL effluent, highlights the importance of catalyst concentration in enhancing photocatalytic efficiency. This finding aligns with previous studies demonstrating that proper dosage of catalysts directly impacts degradation rates of organic pollutants[21,29].

The choice of using natural sunlight for the photocatalytic degradation process, rather than visible light, is supported by the ability of sunlight to provide a broader spectrum of light, including UV rays, which are crucial for activating ZnO NPs. While visible light can initiate some photocatalytic processes, the UV component of sunlight is essential for generating the reactive oxygen species (ROS) necessary for breaking down complex organic molecules found in industrial effluents. The use of natural sunlight not only enhances the photocatalytic activity but also aligns with sustainable practices by reducing reliance on artificial light sources[20].

In this study, the analysis of pH influence on effluent degradation revealed that initial pH values of 10.2 and 10.0 for WSCETP and WSPL, respectively, were optimal for chemical oxygen demand (COD) reduction. Such results are corroborated by the literature indicating that photocatalytic processes are sensitive to pH changes, which can affect the surface charge of catalysts and the speciation of contaminants. The final pH post-treatment (8.4 for WSCETP and 7.2 for WSPL) suggests that the treatment process is effective and results in conditions conducive to subsequent biological degradation,

emphasizing the viability of utilizing ZnO NPs in a dual approach for wastewater treatment[31].

Moreover, the photocatalytic efficiency of ZnO NPs synthesized via green methods has been well-documented in the literature, showcasing the advantages of using natural materials for nanoparticle synthesis. The results of this study further support these findings, as the synthesized ZnO NPs displayed promising degradation rates of various organic pollutants.

Additionally, the role of surface defects in ZnO nanoparticles has been recognized as crucial for enhancing photocatalytic activity, as it can improve charge separation and increase the generation of ROS. Future investigations should explore the correlation between surface morphology and defect density in synthesized ZnONPs to optimize their photocatalytic performance.

CONCLUSION

The synthesized ZnONPs using *Moringa oleifera* Lam demonstrate outstanding photocatalytic properties for the degradation of WSCETP and WSPL effluents. Characterization techniques confirmed the successful synthesis and high purity of ZnONPs, with a band gap of 3.06 eV facilitating effective UV light absorption and ROS generation. Photocatalytic experiments highlighted optimal catalyst loadings of 7.5 g/L for WSCETP and 10 g/L for WSPL, achieving significant COD reductions. Recyclability tests demonstrated that ZnONPs retain substantial photocatalytic activity over multiple cycles, rendering them a feasible and economical choice for effluent treatment. This research underscores the potential of ZnONPs synthesized through eco-friendly methods for efficient and sustainable effluent management, contributing to improved water quality and environmental protection.

ACKNOWLEDGEMENT

The authors sincerely thank CETP (Thane-Belapur) association, Navi Mumbai, and Padmaja Aerobiologicals Pvt. Ltd., Turbhe, Navi Mumbai for delivering the effluent water sample. The authors gratefully acknowledge Ramnarain Ruia Autonomous College for their invaluable resources and technical support throughout this project.

Conflict of interest

All authors stated that there are no competing interests.

REFERENCES

1. Ahmad, F.; Nisar, S. and Mehmood, M., A Critical Review on the Photo Degradation of Diazinon, A Persistent Organic Pesticides. *Journal of the Chemical Society of Pakistan*., **2022**, *44*(5).
2. Akintelu, S.A. and Folorunso, A.S., A review on green synthesis of zinc oxide nanoparticles using plant extracts and its biomedical applications., *BioNanoScience*., **2020**, *10*(4), 848-863.
3. Akram, R.; Fatima, A.; Almohaimeed, Z.M.; Farooq, Z.; Qadir, K.W. and Zafar, Q., Photocatalytic degradation of methyl green dye mediated by pure and Mn-doped zinc oxide nanoparticles under solar light irradiation., *Adsorption Science & Technology*., **2023**, 5069872.
4. Basavanagoudra, H.; Jangannanavar, V.D.; Patil, M.K.; Inamdar, S.R. and Goudar, K.M., Barium oxide nanorods: Catalyst concentration and surface defects' role in degrading methylene blue organic pollutant., *Chemical Physics Impact*., **2024**, *8*, 100578.
5. Borges, M.E.; Sierra, M.; Cuevas, E.; García, R.D. and Esparza, P., Photocatalysis with solar energy: Sunlight-responsive photocatalyst based on TiO_2 loaded on a natural material for wastewater treatment., *Solar Energy*., **2016**, *135*, 527-535.
6. Chemingui, H.; Mzali, J.C.; Missaoui, T.; Konyar, M.; Smiri, M.; Yatmaz, H.C. and Hafiane, A., Characteristics of Er-doped zinc oxide layer: application in synthetic dye solution color removal., *Sep. Purif. Technol*., **2021**, *209*, 402-413.
7. Dhandapani, P.; Prakash, A.A.; AlSalhi, M.S.; Maruthamuthu, S.; Devanesan, S. and Rajasekar, A., Ureolytic bacteria mediated synthesis of hairy ZnO nanostructure as photocatalyst for decolorization of dyes., *Materials Chemistry and Physics*., **2020**, *243*, 122619.

8. Fath, B.D. and Jorgensen, S.E. eds., **2020**. Managing global resources and Universal processes. CRC Press.
9. Kareem, M.A.; Bello, I.T.; Shittu, H.A.; Sivaprakash, P.; Adedokun, O. and Arumugam, S., Synthesis, characterization, and photocatalytic application of silver doped zinc oxide nanoparticles., *Cleaner Materials*., **2022**, *3*, 100041.
10. Lallo da Silva, B.; Abuçafy, M.P.; Berbel Manaia, E.; Oshiro Junior, J.A.; Chiari-Andréo, B.G.; Pietro, R.C.R. and Chiavacci, L.A., Relationship between structure and antimicrobial activity of zinc oxide nanoparticles: An overview., *International Journal of Nanomedicine*., **2019**, 9395-9410.
11. Liu, H.; Wang, C. and Wang, G., Photocatalytic advanced oxidation processes for water treatment: recent advances and perspective., *Chemistry–An Asian Journal*., **2020**, *15*(20), 3239-3253.
12. Liu, R.; Fu, X.; Guo, Y.; Zhang, J. and Tian, W., A study on Ag or Ce doped and co-doped ZnO for the photocatalytic degradation of RhB dye., *Vacuum*., **2023**, *215*, 112337.
13. Liu, Y.; Zhang, Q.; Xu, M.; Yuan, H.; Chen, Y.; Zhang, J.; Luo, K.; Zhang, J. and You, B., Novel and efficient synthesis of Ag-ZnO nanoparticles for the sunlight-induced photocatalytic degradation., *Applied Surface Science*., **2019**, *476*, 632-640.
14. Majumder, S.; Chatterjee, S.; Basnet, P. and Mukherjee, J., ZnO based nanomaterials for photocatalytic degradation of aqueous pharmaceutical waste solutions–A contemporary review., *Environmental Nanotechnology, Monitoring & Management*., **2020**, *14*, 100386.
15. Melchionna, M. and Fornasiero, P., Updates on the Roadmap for Photocatalysis., *Acs Catalysis*., **2020**, *10*(10), 5493-5501.
16. Nath, S.; Shyanti, R.K. and Pathak, B., Plant-mediated synthesis of silver and gold nanoparticles for antibacterial and anticancer applications., *Green Nanoparticles: Synthesis and Biomedical Applications*., **2020**, 163-186.
17. Naz, F. and Saeed, K., Investigation of photocatalytic behavior of undoped ZnO and Cr-doped ZnO nanoparticles for the degradation of dye., *Inorganic and Nano-Metal Chemistry*., **2021**, *51*(1), 1-11.
18. Ong, C.B.; Ng, L.Y. and Mohammad, A.W., A review of ZnO nanoparticles as solar photocatalysts: Synthesis, mechanisms and applications., *Renewable and Sustainable Energy Reviews*., **2018**, *81*, 536-551.
19. Perumalsamy, H.; Balusamy, S.R.; Sukweenadhi, J.; Nag, S.; MubarakAli, D.; El-Agamy Farh, M.; Vijay, H. and Rahimi, S., A comprehensive review on Moringa oleifera nanoparticles: importance of polyphenols in nanoparticle synthesis, nanoparticle efficacy and their applications., *Journal of Nanobiotechnology*., **2024**, *22*(1), 71.
20. Ren, G.; Han, H.; Wang, Y.; Liu, S.; Zhao, J.; Meng, X. and Li, Z., Recent advances of photocatalytic application in water treatment: A review., *Nanomaterials*., **2021**, *11*(7), 1804.
21. Saeed, M.; Muneer, M.; Haq, A.U. and Akram, N., Photocatalysis: An effective tool for photodegradation of dyes-A review., *Environmental Science and Pollution Research*., **2022**, *29*(1), 293-311.
22. Sansenya, T.; Masri, N.; Chankhanittha, T.; Senasu, T.; Piriyanon, J.; Mukdasai, S. and Nanan, S., Hydrothermal synthesis of ZnO photocatalyst for detoxification of anionic azo dyes and antibiotic., *Journal of Physics and Chemistry of Solids*., **2022**, *160*, 110353.
23. Senasu, T.; Chankhanittha, T.; Hemavibool, K. and Nanan, S., Visible-light-responsive photocatalyst based on ZnO/CdS nanocomposite for photodegradation of reactive red azo dye and ofloxacin antibiotic., *Materials Science in Semiconductor Processing*., **2021**, *123*, 105558.
24. Shafey, A.M.E., Green synthesis of metal and metal oxide nanoparticles from plant leaf extracts and their applications: A review., *Green Processing and Synthesis*., **2020**, *9*(1), 304-339.
25. Shubha, J.P.; Kavalli, K.; Adil, S.F.; Assal, M.E.; Hatshan, M.R. and Dubasi, N., Facile green synthesis of semiconductive ZnO nanoparticles for photocatalytic degradation of dyes from the textile industry: A kinetic approach., *Journal of King saud University-Science*., **2022**, *34*(5), 102047.
26. Stani, V. and Tanaskovi, S.B., Antibacterial activity of metal oxide nanoparticles., *In Nanotoxicity.,* **2020**, 241-274. Elsevier.

27. Sudhakar, C.; Poonkothai, M.; Selvankumar, T. and Selvam, K., Facile synthesis of iron oxide nanoparticles using Cassia auriculata flower extract and accessing their photocatalytic degradation and larvicidal effect., *Journal of Materials Science: Materials in Electronics*., **2022**, *33*(14), 11434-11445.
28. Tripathy, J.; Mishra, A.; Pandey, M.; Thakur, R.R.; Chand, S.; Rout, P.R. and Shahid, M.K., Advances in Nanoparticles and Nanocomposites for Water and Wastewater Treatment: A Review. *Water*., **2024**, *16*(11), 1481.
29. Waghchaure, R.H.; Adole, V.A. and Jagdale, B.S., Photocatalytic degradation of methylene blue, rhodamine B, methyl orange and Eriochrome black T dyes by modified ZnO nanocatalysts: A concise review. *Inorganic Chemistry Communications*., **2022**, *143*, 109764.
30. Weldegebrieal, G.K., Synthesis method, antibacterial and photocatalytic activity of ZnO nanoparticles for azo dyes in wastewater treatment: A review. *Inorganic Chemistry Communications*., **2020**, *120*, 108140.
31. Zheng, A.L.T.; Abdullah, C.A.C.; Chung, E.L.T. and Andou, Y., Recent progress in visible light-doped ZnO photocatalyst for pollution control., *International Journal of Environmental Science and Technology*., **2023**, *20*(5), 5753-5772.